

# Initial Test Results from the Palomar 200" Adaptive Optics System

R. Dekany<sup>a</sup>, K. Wallace<sup>a</sup>, G. Brack<sup>a</sup>, B. R. Oppenheimer<sup>b</sup>, D. Palmer<sup>a</sup>

<sup>a</sup> Jet Propulsion Laboratory  
Spatial Interferometry Systems Group  
4800 Oak Grove Blvd.  
Pasadena, CA 91109

<sup>b</sup> Palomar Observatory  
105-24 California Institute of Technology  
Pasadena, CA 91125

## ABSTRACT

We present laboratory subsystem test results obtained during integration of the Palomar 200" Adaptive Optics System at Jet Propulsion Laboratory. These results pertain to the 241 actively controlled actuator, Shack-Hartmann sensed, initial delivery of a system optimized for near infrared observation with the 5 meter diameter telescope at Palomar Mountain. This system initially exploits natural guide stars. Our intention is to provide a wide-ranging summary of subsystem performance measurements and several lessons learned. Noteworthy among these results is our measurement of  $6.3 \pm 0.2$  electron read noise performance of our initial WFS camera, based upon a 64 x 64 pixel MIT/LL CCD detector, running at 600 kilopixel per sec per output amplifier. This camera was constructed by SciMeasure Analytical Systems, Inc. of Decatur, GA.

**Keywords:** Adaptive optics, infrared instrumentation, wavefront sensing, large telescope instrumentation

## 1. INTRODUCTION

The Palomar 200" AO system<sup>1</sup> has been undergoing integration at Jet Propulsion Laboratory (JPL) since February 1997. The last major subsystem, the wavefront sensor camera, was received on June 12, 1997, and we are currently involved in integration and end-to-end system testing of the instrument. A mechanical and electrical interface test is planned for the instrument at the 200" telescope this July. Initial closure of the adaptive loop on the sky ("first lock") is scheduled for December 1997. At approximately the same time, collaborators at Cornell University are scheduled to deliver a new near-IR camera system<sup>2</sup> optimized for use with the AO instrument. Commissioning of the AO system and camera as facility instruments at Palomar is expected in the Fall of 1998.

As a reference for the discussions to follow, Figure 1 contains an overview of the instrument layout, as seen by an observer looking through the optical bench. Note that the optical components of the AO system and the IR camera mount to the underside of the optical bench, which in turn mounts to the Cassegrain ring of the telescope. In comparison to this, Figure 2 contains a photograph of the optical bench, as taken from the corner of the instrument containing the folding mirror labeled FM3. Note that relative to Figure 1, the optical bench has been inverted in its turnover jig for the photo in Figure 2, resulting in an apparent change in layout symmetry.

---

Further author information -  
R.D.(correspondence): Email: [dekany@huey.jpl.nasa.gov](mailto:dekany@huey.jpl.nasa.gov); WWW: <http://huey.jpl.nasa.gov/AO/>

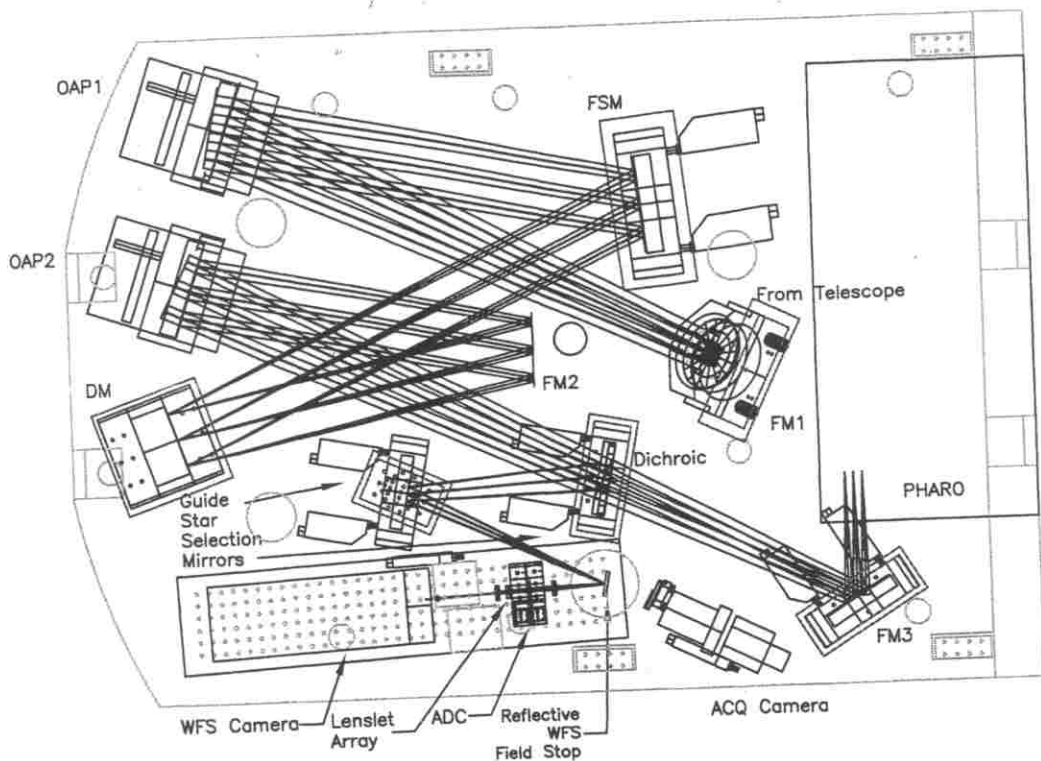


**Figure 1.** A combination Zemax ray-trace and AutoCAD drawing of the Palomar 200" Adaptive Optics System, as seen from above, as if looking through the optical bench when mounted at Cassegrain. Light beyond Cass focus passes through the optical bench and is diverted into the table plane by a 45 degree fold mirror (FM1), collimated by an off-axis parabolic mirror (OAP1), tilted by the fast steering mirror (FSM), corrected by the deformable mirror (DM) and reimaged by OAP2. IR light passes through a dichroic and is folded by FM3 to the science camera, while visible light reflects off the dichroic and star selection mirror before encountering a reflective spot at the relay focus that serves as a field stop for the wavefront sensor (WFS). Light striking this spot is collimated within the WFS, passes through an atmospheric dispersion corrector (ADC), is subdivided by the lenslet array and reimaged onto the WFS camera. Light missing the field stop is reimaged onto an aquisition camera (ACQ). The field of view of the AO relay is 45 arcseconds radius, the WFS field stop is square with edge length of 4 arcseconds, and the FSM has a range of  $\pm 2$  arcseconds, all referenced to the sky.

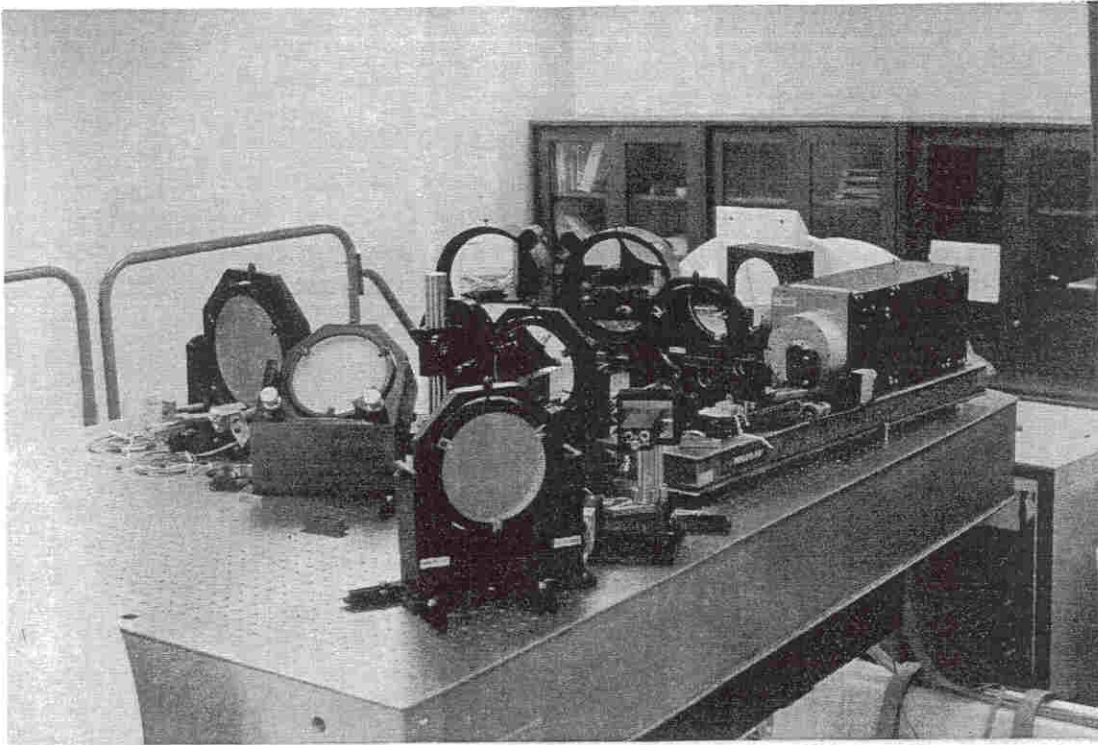


**Figure 2.** The Palomar AO system undergoing integration at Jet Propulsion Laboratory. In this view, the instrument is held within a rotating jig used to test for system flexure. FM3 is in the foreground, FSM is left, and the WFS is right. For comparison with Figure 1, the instrument has been inverted within the jig. The stimulus mounts on the opposite side of the optical bench from these optics.

## 2. OPTOMECHANICAL TEST RESULTS

During the past 9 months, a series of component and subsystem tests have been performed at JPL. In this section, we briefly summarize key performance measures of several subsystems.

### 2.1 Optical components and alignment

During the design of the AO instrument, our allocation of optical error budget to individual component selection and tolerancing was conducted to ensure that the total amount of deformable mirror (DM) stroke used to correct internal static aberrations remained less than 5% of the total stroke available (note that the results of our investigation of our Xinetics, Inc. 349 actuator deformable mirror<sup>3</sup> is presented elsewhere<sup>4</sup>). Given 4 microns of DM actuator stroke, this requirement set an instrument optical error budget of 400 nm P-V wavefront. This is much smaller than the known 1-2  $\mu\text{m}$  P-V wavefront aberrations apparent in the Hale primary mirror when observing at large zenith angles. (In preparation for the commissioning of the AO system, Palomar Observatory has undertaken an extensive program of mirror support improvements and environment control to reduce the DM stroke expended correcting local sources as well as improve seeing conditions for the other facility instruments.)

We distributed the instrument wavefront error budget through the optical system as follows:

Off-axis parabola wavefront error	120 nm each (2)
Flat mirror wavefront error	120 nm each (5)
Dichroic mirror wavefront error	150 nm
WFS internal wavefront errors	100 nm
Alignment errors	150 nm
<hr/>	
Total P-V (added in quadrature)	400 nm

This allotment allowed us to specify  $\lambda/10$  P-V optics, which are readily available at modest cost. The dichroic mirror entry in the above table is due to our use of the dichroic beamsplitter (a plane parallel plate) in a converging beam, which introduces astigmatism (in addition to longitudinal color) in the science arm of the instrument. Each of the optical components were acceptance tested and found to meet the above specification, except for the 8" diameter off-axis parabolas (OAPs) manufactured by Space Optics Research Laboratory (SORL), which were found to be  $\lambda/8$  ( $\lambda = 633\text{nm}$ ) over the 90% clear aperture. However, because several of the flat mirrors were determined to enjoy better surface quality than specified, we elected to accept the OAPs as delivered. All the optical acceptance tests showed little static aberrations on spatial scales smaller than the DM actuator spacing. From this, we believe that the 400 nm of static wavefront error allocated for the AO system can be internally corrected to better than 20 nm P-V using the deformable mirror.

We have also performed a series of flexure tests in our laboratory using the rotation provided by our inversion fixture (see Figure 2). We have found flexure of the optical bench, manufactured by Technical Manufacturing Company (TMC), negligible compared to the flexure due to our optical mounts. (Selection of TMC as the optical bench manufacturer was based largely on cost). We suspect the majority of the flexure is due to a single post-mounted mirror and are investigating improving its stiffness. Aside from this post mount, we suspect the next major contributor to flexure are our OAP mounts procured from SORL, which we have been forced to modify twice to accommodate inversion.

To simulate the effect of a one hour science exposure, we rotated the instrument from its zenith-looking position over 15 degrees, and measured the total and non-common image motion. The optical mounts were found to induce approximately 1.5 arcseconds of total flexure induced image motion at the IR focal plane. Of this motion, however, the majority is common path to both the science camera and the WFS, and will be corrected during closed loop operation. Over the same 15 degree rotation, we have measured the non-common image motion to correspond to approximately 200 milliarcseconds (mas) on the sky. Although small compared to the imaging capability of most current astronomical instrumentation, this is large compared to the K-band diffraction limited image width of 90 mas, and much larger than our science-driven goal of less than 10 mas uncorrected error during a one hour exposure.

We believe the thermal and long-term mechanical stability of our optical mounts will result in a non-calibratable residual error that is large compared to 10 mas (which corresponds to approximately 3 microns of lateral motion at our F/15.7 science focus). Even with sufficient thermal stability, calibration at these levels is expensive in terms of the time necessary to measure flexure induced image motion with sufficient fidelity and sampling across the sky. Because of this expense, we are planning the addition of a laser metrology system<sup>1</sup> to monitor the otherwise unsensed image motion between the science arm and the WFS arm of the instrument.

The optical throughput of the instrument, from first folding mirror to the WFS field stop, has been measured to be 67% for HeNe laser light, corresponding to 95% reflectance from each of the reflections coated with protected Ag (Denton FSS-99 or similar). Note that additional losses in the telescope and WFS are expected to result in approximately 30% transmission (for clean optics) from guide star to WFS detector. So far, an IR source and detector have not been available to measure the infrared throughput.

## 2.2 Stimulus

Critical to the integration and automation of the AO system is a subsystem we refer to as the stimulus. Several capabilities are provided within the stimulus to aid in the operation of the instrument. These capabilities include:

1) A phase-shifting interferometer, used in conjunction with one of several slide-in mirrors to rapidly interrogate the optical wavefront quality of the AO relay, or to evaluate the status of the deformable mirror actuators.

2) A telescope simulator, aligned to the 200" telescope during an engineering run last October. The boresight and pupil internal to the stimulus matches that of the telescope to within an arcsec equivalent on the sky, and is being used to align the AO relay.

3) A turbulator, which can introduce phase errors within the stimulus beam for system testing. The turbulator is placed on a motorized stage beneath a converging beam, which allows the spatial scales present within the turbulence to be varied automatically. Our turbulator design is heater based, which eliminates the need for consumables, such as required for low density gas based turbulence generators.

4) A metrology source used in the automated calibration of the deformable mirror centroid sensitivity matrix and for a phase diversity based non-common-path wavefront calibration scheme.

5) A physical standoff of the instrument to the Cass ring, to allow for free rotation of the instrument about the telescope axis, for use with a slit spectrograph<sup>2</sup>.

## 2.3 Fast steering mirror

The combination of relay focal ratio, the DM actuator spacing, and packaging constraints imposed upon the AO instrument by the Cassegrain environment led to the need to incorporate an 8" diameter fast steering mirror (FSM) into the 200" AO system. The FSM was constructed through modification of an Aerotech AOM-8 optical mount to accept two long-throw (40um) PZT actuators, yielding tip/tilt control of approximately  $\pm 2$  arcsec on the sky.

Because of this mirror's large size, we were somewhat concerned with the mechanical properties of the Aerotech mount. Accelerometer tests of the AOM-8 were conducted using an aluminum disk in place of the Zerodur optic. We determined that the fundamental resonant "flopping" mode of the outer gimbal ring is excited at a frequency of 60 Hz. Because tip and tilt aberrations over the 5 meter telescope are rather benign, we have baselined a 50 Hz update rate for the FSM control loop. In order to provide some design margin, we plan to stiffen the outer gimbal ring later this summer to raise its fundamental resonance to about 100 Hz. Favorable experience retrofitting similar mounts makes us optimistic this can be straightforwardly achieved.

## 2.4 Wavefront sensor

The 200" AO system wavefront sensor is based upon a conventional Shack-Hartmann architecture. Unlike previous systems utilizing a quad cell centroid detection, however, our wavefront sensor subaperture images are detected within a 4 x 4 pixel region of the CCD, utilizing a two-stage centroiding algorithm, suggested by Goad<sup>5</sup>. Fundamentally, the first stage of the centroid calculation is used to access a lookup table containing optimal filters used in the second stage calculation. This provides near optimum noise performance with increased dynamic range of the sensor.

In order to facilitate maintenance and easy exchange between the current WFS camera and subsequent cameras arriving during the system development, the WFS is implemented on a removable breadboard that remains internally aligned when installed or taken off the AO bench. An Adaptive Optics Associates rectangular format lenslet array with 400um pitch and 25 mm focal length is used to sense tilts over 16 subapertures across the demagnified 6.4 mm diameter pupil, yielding a total of 241 sensed subapertures (less those obscured by the telescope secondary). The optical distortion apparent in the subaperture images as relayed onto the CCD is less than 2%. This corresponds to approximately 15% of

the worst-case subaperture width and is calibrated (at the cost of reducing centroid dynamic range within those subapertures). A photograph of the WFS subsystem undergoing alignment with a single mode fiber laser source is shown in Figure 3.

#### 2.4 Wavefront sensor camera

JPL has pursued several parallel paths for the development of a low-noise wavefront sensor (WFS) camera. Our philosophy has been to procure a state-of-the-art low noise commercial camera system from SciMeasure Analytical Systems, Inc. while simultaneously exploring lower noise alternative designs. The initial camera system is based upon a 64 x 64 pixel science format MIT/LL CCID-19 fast frame rate chip, with sampling rates as high as 600 Hz. SciMeasure has also been funded to provide a low-noise camera based upon an EEV39 CCD. We continue to explore the potential of our JPL-developed "skipper" chip<sup>6</sup>, albeit at low level due to funding constraints, and administer an SBIR with PixelVision, Inc. for the development of advanced high frame rate array detectors.

The first element of this strategy was realized in June 1997, with the delivery of the MIT/LL based WFS camera from SciMeasure to JPL. Since receipt of the camera, we have measured the read noise of this 4 output amplifier device at 600 Hz frame rate (or about 600 Kpix/sec/channel), operating at a chip temperature of -19C. We have measured the read noise<sup>7</sup> to vary between 6.1 to 6.5 e- RMS, depending on the output amplifier channel. This very nearly matches the noise performance of  $6.1 \pm 0.2$  e- RMS measured by SciMeasure prior to shipping. Although this result is promising, we look forward to evaluating the camera's noise performance in the telescope environment during our engineering run next month.

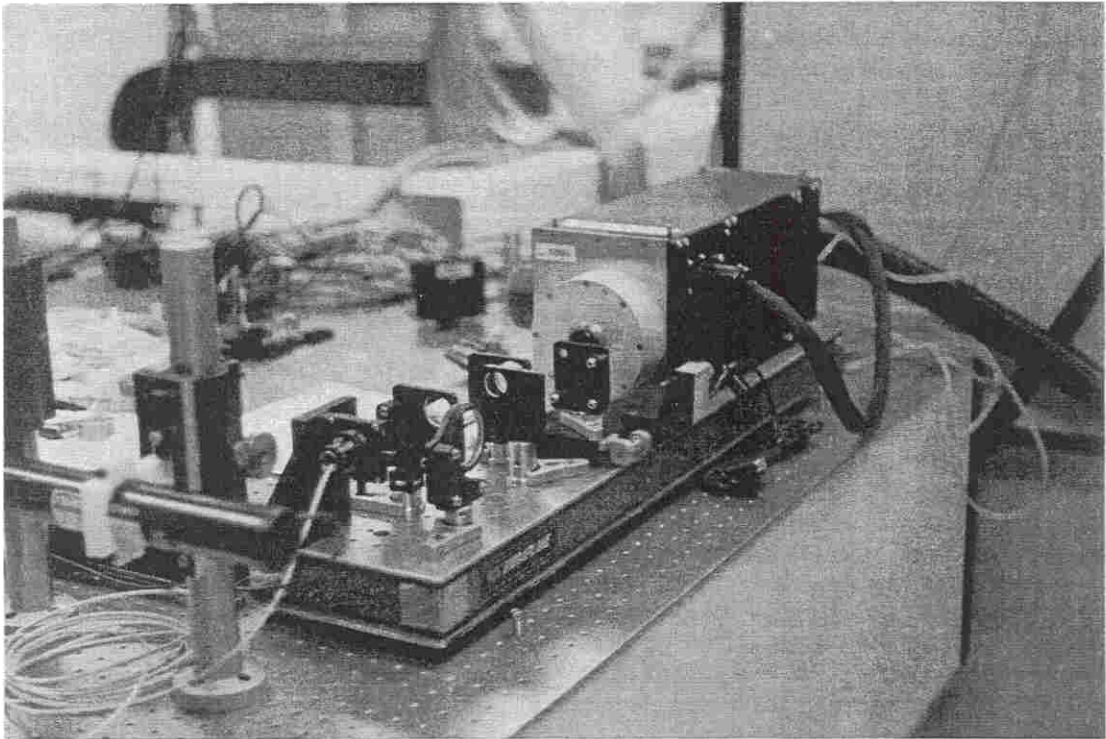


**Figure 3.** The Palomar AO instrument wavefront sensor breadboard. In this view, the WFS field stop (a small reflecting spot on a BK7 substrate) has been replaced by a single mode optical fiber for subsystem alignment. Then, proceeding away from the viewer are a collimating lens, the atmospheric dispersion corrector (not in place for these tests), the lenslet array, and two reimaging lenses to match the lenslet pitch to the subaperture (4 pixel) pitch on the WFS camera.

### 3. BENCHMARKING

The computing workhorse of the 200" AO system is a DSP engine utilizing 9 Texas Instruments C40 processors, implemented in a pipelined architecture<sup>1</sup>. Data from the four WFS camera output channels are directed via a custom board into 4 centroiding DSPs utilizing the DSP commport interface. Centroid calculation begins as soon as 64 pixels are received by a centroiding DSP. Centroids are sent again via commport interface to 4 reconstruction DSPs, which begin their reconstruction calculation once 4 centroids have been received.

For testing and benchmarking the DSP engine, prior to receipt of the WFS camera itself, we developed a WFS camera emulator. The camera emulator simulates in hardware the data flow from the WFS camera. The emulator is implemented on a spare CV4 carrier board, containing 4 additional C40 DSPs. Simulated WFS camera pixel data is generated on our UltraSparc, and then loaded into the emulator DSP memory. The emulator then sends this pixel data to the actual centroiding DSPs, and generates an emulated camera frame synch over the VME backplane that synchronizes the compute pipeline processing. In this manner, up to 1000 simulated camera frames can be sent through the wavefront processor pipeline at up to 500 Hz.

Benchmarking of the wavefront processor (WFP) pipeline has verified the timing diagram for the pipelining process, shown in Figure 4. We have found that the latency within the pipeline to be 2.7 millisecond. Operating the WFS camera with 2 ms exposure time results in a mean data age of the adaptive correction of 3.7 ms.

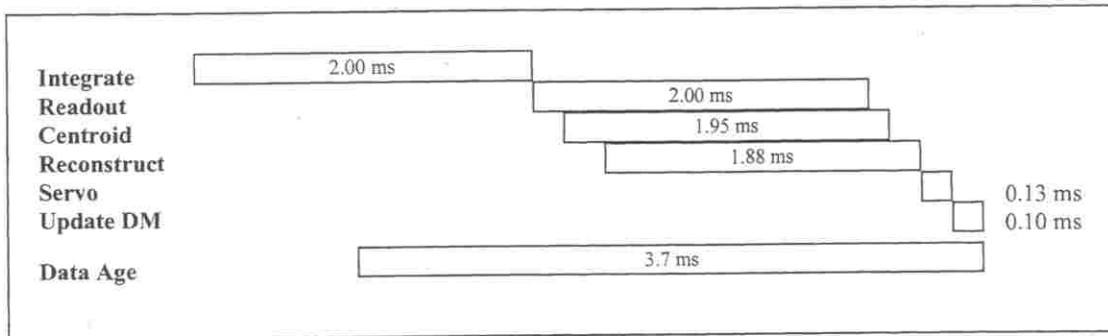


**Figure 4.** Timing diagram for the wavefront processor pipeline used within the Palomar AO instrument. This diagram corresponds to 500 Hz WFS sampling of our current 64 x 64 pixel CCD and a pipelined centroiding and reconstruction calculation using 9 TI C40 DSPs.

### ACKNOWLEDGEMENTS

This work is being performed at the Jet Propulsion Laboratory, California Institute of Technology, under a contract with the National Aeronautics and Space Administration.

## REFERENCES

- <sup>1</sup> Dekany, R., "The Palomar Adaptive Optics System", OSA 1996 Adaptive Optics Topical Meeting Proceedings, pg. 40, Optical Society of America, (1996).
- <sup>2</sup> Brandl, B., Hayward, T., and Houck, J., "PHARO (Palomar High Angular Resolution Observer): a dedicated NIR camera for the Palomar adaptive optics system", SPIE Proceedings, 3126, (1997).
- <sup>3</sup> Ealey, M., and Wellman, J., "Xinetics Low Cost Deformable Mirrors with Actuator Replacement Cartridges", SPIE Proceedings, 2201, 680 (1994).
- <sup>4</sup> Oppenheimer, B. R., Palmer, D., Dekany, R., Sivaramakrishnan, A., Ealey, M., and Price, T., "Investigating a Xinetics, Inc. Deformable Mirror", SPIE Proceedings, 3126, (1997).
- <sup>5</sup> Goad, L., "Digital image centering," SPIE Proceedings, 627, 688 (1986).
- <sup>6</sup> Levine, B. M., Janesick, J., and Shelton, J. C., "Development of a low noise high frame rate CCD for adaptive optics", SPIE Proceedings, 2201, 596 (1994).
- <sup>7</sup> McLean, I. S., Electronic Imaging in Astronomy, Praxis Publishing Ltd, Chichester, 1997.